MCTP-16-25

Implications of a Stop Sector Signal at the LHC

Aaron Pierce[1] and Bibhushan Shakya[2,1]

[1] *Michigan Center for Theoretical Physics,*
University of Michigan, Ann Arbor, MI 48109, USA

[2] *Department of Physics, University of Cincinnati, Cincinnati, OH 45221, USA*

arXiv:1611.00771v1 [hep-ph] 2 Nov 2016

Abstract

Naturalness arguments suggest that the stop sector is within reach of the Large Hadron Collider (LHC). We investigate how the observation of a third generation squark signal could predict masses and discovery modes of other supersymmetric particles, or potentially test the Higgs boson mass relation and the validity of the Minimal Supersymmetric Standard Model (MSSM). We illustrate these ideas in three distinct scenarios: discovery of a light stop, a sbottom signal in multileptons, and a signal of the second (heavier) stop in boosted dibosons.

I. INTRODUCTION AND MOTIVATION

If the electroweak scale is natural, third generation squarks should be among the first supersymmetric particles to be discovered at the Large Hadron Collider (LHC). The latest results from Run II of the LHC place strong limits on their masses under various assumptions about the mass spectrum and decay channels [1–9]. Nevertheless, windows for light ($\lesssim$ TeV) third generation squarks still exist, and there have even been recent hints of signals of such light states (e.g. [10, 11]). The discovery of a third generation squark at the LHC in the next few years remains an exciting possibility.

Such a discovery carries important implications, both theoretical and observational. One of the primary appeals of a stop sector discovery is that it is intricately tied to the mass of the Higgs boson [12–14]. Given the measurements of the mass and properties of the Higgs in recent years, this connection provides strong constraints on the possible values of stop masses and mixing, which, in turn, determine their decay branching ratios. Furthermore, the left-handed stop is part of a doublet that also contains the left-handed sbottom, hence their masses are related: in particular, after mixing in the stop sector, the left-handed sbottom mass lies between the two stop mass eigenstates provided sbottom mixing is not too large. Such correlations imply that an initial signal can enable predictions of subsequent signals at the LHC. Establishing discrepancies between the observed Higgs mass and that predicted from third generation sparticle measurements could rule out the Minimal Supersymmetric Standard Model (MSSM) as the underlying theory behind these signals, establishing the need for a non-minimal version of supersymmetry, such as the Next-to-Minimal Supersymmetric Standard Model (NMSSM). Such predictions and consistency checks can remain largely insensitive to the remainder of the supersymmetric mass spectrum.

In this paper, we study such theoretical and observational implications of a stop sector signal at the LHC within a few specific scenarios. These are not intended to provide comprehensive coverage of all possibilities, but rather offer qualitative illustrations of the various ways in which progress can be made once a signal is observed.[1] In the event of a relevant discovery of the type described here, it would be of interest to carry out the corresponding theory calculations with higher precision (i.e. higher loop level) and examine the collider aspects (i.e. event and

[1] Earlier ideas using measurements to constrain parameters in the stop sector include [15, 16].

background simulations) with additional care.

Following a review of the basic theoretical framework and relevant observational constraints in Sec. II, we study how the Higgs mass relation can be used to perform consistency checks on the entire MSSM framework, or alternatively predict masses and decay modes of other superpartners, in three distinct scenarios. In Sec. III, we investigate how predictions can be made for sbottom or heavier stop masses and decay modes following a light stop discovery. Sec. IV investigates how information about the heavier stop can be deduced from measurements of a sbottom signal in multileptons. In Sec. V, we study how measurements of the heavier stop decay in boosted diboson channels can be used to test the consistency of the MSSM Higgs mass relation and either corroborate or rule out the MSSM.

II. THEORETICAL FRAMEWORK

We denote the lighter and heavier stop mass eigenstates as $\tilde{t}_1$ and $\tilde{t}_2$ respectively. We denote the stop mixing angle as θ_t, with $\tilde{t}_1 = \cos\theta_t\,\tilde{t}_L + \sin\theta_t\,\tilde{t}_R$, where $\tilde{t}_L$, $\tilde{t}_R$ are the stop gauge eigenstates, so that $\theta = 0$ corresponds to the scenario where the lighter stop is left-handed. In terms of these parameters, the Higgs boson mass at one-loop in the MSSM is [17]

$$m_h^2 = m_Z^2\cos^2(2\beta) + \frac{3\sin^2\beta\, y_t^2}{4\pi^2}\,[\, m_t^2 \ln\left(\frac{m_{\tilde{t}_1} m_{\tilde{t}_2}}{m_t^2}\right) + c_t^2 s_t^2 (m_{\tilde{t}_2}^2 - m_{\tilde{t}_1}^2)\ln\left(\frac{m_{\tilde{t}_2}^2}{m_{\tilde{t}_1}^2}\right) + c_t^4 s_t^4 \left\{ (m_{\tilde{t}_2}^2 - m_{\tilde{t}_1}^2)^2 - \frac{1}{2}(m_{\tilde{t}_2}^4 - m_{\tilde{t}_1}^4)\ln\left(\frac{m_{\tilde{t}_2}^2}{m_{\tilde{t}_1}^2}\right)\right\} / m_t^2\,], \tag{1}$$

where $s_t(c_t) = \sin\theta_t(\cos\theta_t)$. For $\tan\beta$ sufficiently large that $\cos^2(2\beta) \approx 1$, but not so large that (s)bottom loops are significant, the Higgs boson mass at one-loop is therefore determined by the three parameters $m_{\tilde{t}_1}$, $m_{\tilde{t}_2}$, and θ_t.

For degenerate stops, the logarithmic stop correction in the first term in the square parenthesis is dominant. In this degenerate scenario, increasingly heavy stops masses can be made consistent with the measured Higgs mass $m_h = 125$ GeV by appropriately decreasing the tree-level contribution to match the increasing loop contribution. However, as the mass splitting between the two stops increases, the remaining two terms in the loop correction grow stronger. A key observation is that the final term switches sign and becomes negative for $m_{\tilde{t}_2} \gtrsim 2.7 m_{\tilde{t}_1}$. For non-vanishing stop mixing and $m_{\tilde{t}_2} \gg m_{\tilde{t}_1}$, this negative term can dominate. Therefore, for

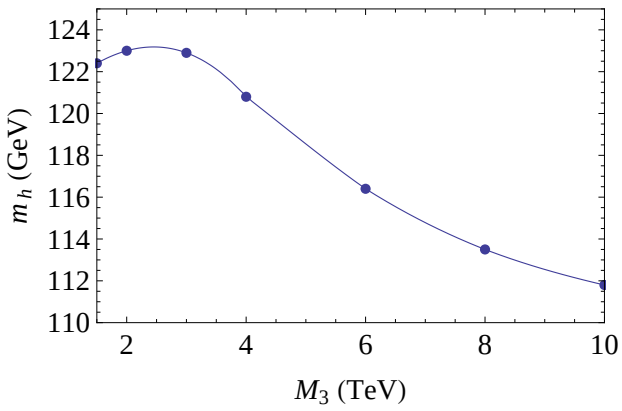

FIG. 1. Higgs mass dependence on the gluino mass parameter M_3 for $m_{\tilde{t}_2} = 851$ GeV, $m_{\tilde{t}_1} = 459$ GeV, and $\sin\theta_t = 0.724$, as calculated with `SUSY-HIT` [18].

nonzero mixing, there exists an *upper* limit on $m_{\tilde{t}_2}$ (as a function of $\tilde{t}_1$ and θ_t), beyond which it is impossible to accommodate $m_h = 125$ GeV in the MSSM. In other words, a measurement of $m_{\tilde{t}_1}$ and some knowledge of θ_t allows for an upper limit on $m_{\tilde{t}_2}$. Ruling out $m_{\tilde{t}_2}$ in this window rules out the MSSM. This statement is independent of the rest of the supersymmetric spectrum at one-loop (see related discussion below). In this case, one can conclude that the supersymmetric theory must include additional corrections to the Higgs mass, as, for instance, in the Next-to-Minimal Supersymmetric Standard Model (NMSSM). Thus, even partial information on the three parameters $m_{\tilde{t}_1}$, $m_{\tilde{t}_2}$, and θ_t can suffice to make meaningful statements about the underlying supersymmetric model.

In this paper, we will make use of the analytic one-loop formula in Eq. (1) to calculate the Higgs mass. This is a crude approximation, but sufficient to illustrate our main ideas. We take the $120 \leq m_h \leq 130$ GeV mass window as potentially compatible with the measured mass of the Higgs boson; we allow this generous 10 GeV window to account for several corrections not captured by this simple formula, which are known to amount to a few GeV. For example, the Higgs mass is sensitive to both the uncertainty in and the running of the top Yukawa (we use $m_t = 173$ GeV); these are known to affect the Higgs mass by a few GeV [19–21]. Likewise, at higher loop order the Higgs mass is sensitive to the gluino mass, particularly for large stop mixing. Assuming the gluino is not too heavy (remains $\lesssim 4$ TeV), we find that the associated uncertainly in the Higgs mass remains a few GeV. We illustrate this dependence for a specific choice of stop masses and mixing angle in Fig. 1 (see also Ref. [22] for a more detailed study; its

results are in agreement with the above statement). For very heavy gluinos, $\mathcal{O}(10)$ TeV, the Higgs mass rises logarithmically with the gluino mass (see Ref. [22]), and it might be possible to recover the correct Higgs mass with such a spectrum. However, it is difficult to motivate a scenario where the gauginos are much heavier than the squarks, and we do not pursue this direction further. Varying $\tan\beta$ over the range $15 \leq \tan\beta \leq 40$ does not change the Higgs mass by more than ~ 1 GeV. The 10 GeV window of uncertainty is broad enough to encompass all of these factors.

The left-handed sbottom is inextricably linked with the stop sector as it is part of a doublet with the left-handed stop. For simplicity, we decouple the right-handed sbottom from our analysis. In this case, the lighter sbottom is purely left-handed; in terms of the parameters we are working with, its mass can then be written as

$$m_{\tilde{b}_1}^2 = m_{\tilde{t}_2}^2 \sin^2\theta_{\tilde{t}} + m_{\tilde{t}_1}^2 \cos^2\theta_t - m_t^2 + m_W^2. \tag{2}$$

Thus the lighter sbottom mass is fixed by the same three parameters that fix the Higgs mass, providing another constraint in the system. The upper limit discussed above for $m_{\tilde{t}_2}$ (imposed by the Higgs boson mass) can also be translated to an upper limit on $m_{\tilde{b}_1}$.

A. Indirect Constraints on Light Stops

To appreciate the range of possible LHC signals, it is useful to first discuss indirect constraints on light third generation squarks. In particular, when stop mixing is significant, as might be suggested by the Higgs boson mass if the stops are light, there can be significant contributions to the ρ parameter or a modification of the Higgs boson production rate.

The one-loop contribution to the ρ parameter is [23–26]

$$\Delta\rho = \frac{3\,G_F}{8\sqrt{2}\pi^2}\left[-s_t^2\,c_t^2\,F_0(m_{\tilde{t}_1}^2, m_{\tilde{t}_2}^2) + c_t^2\,F_0(m_{\tilde{t}_1}^2, m_{\tilde{b}_1}^2) + s_t^2\,F_0(m_{\tilde{t}_2}^2, m_{\tilde{b}_1}^2)\right], \tag{3}$$

where

$$F_0(x,y) = x + y - \frac{2xy}{x-y}\log\frac{x}{y}. \tag{4}$$

We take the constraint from Ref. [27], $\Delta\rho = (4.2 \pm 2.7)\times 10^{-4}$. We demand consistency with this number to 2σ. In general, $\Delta\rho$ increases as the mass eigenstates get more split or as the mixing becomes larger. However, as discussed earlier, a large mass splitting with large mixing

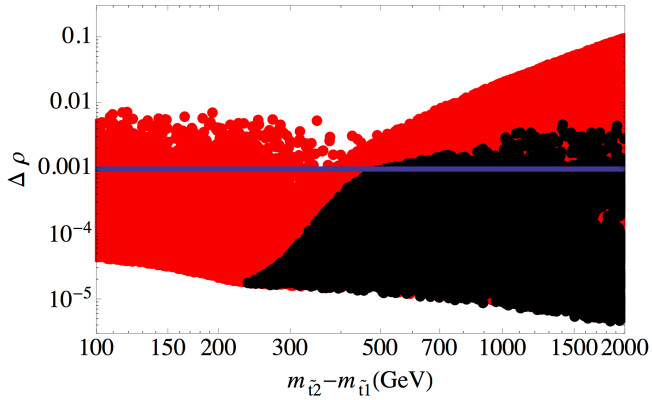

FIG. 2. $\Delta\rho$ for all scanned points (red) and those compatible with $120 < m_h < 130$ GeV (black), as a function of the mass splitting between the two stop mass eigenstates. All points have $m_{\tilde{t}_1} < 1$ TeV. The horizontal blue line denotes $\Delta\rho = 9.6 \times 10^{-4}$, the 2σ upper limit from measurements.

suppresses the Higgs boson mass on account of the large negative term in the loop contribution. Indeed, for $m_{\tilde{t}_1} < 1$ TeV, we find that points with the correct Higgs mass are correlated with small values of $\Delta\rho$. These features are shown in Fig. 2.

The existence of a light stop can also modify the Higgs-gluon-gluon coupling, which is constrained to be somewhat close to its Standard Model (SM) value. The stop contribution to this coupling is [28, 29]

$$r_{gg} \equiv \kappa_g^2 \equiv \frac{\Gamma(h \to gg)}{\Gamma(h \to gg)_{SM}} = \left(1 + \frac{1}{A_{hgg(SM)}} \left[\frac{\lambda_{ht_1t_1} A_0[m_{\tilde{t}_1}]}{{m_{\tilde{t}_1}}^2} + \frac{\lambda_{ht_2t_2} A_0[m_{\tilde{t}_2}]}{{m_{\tilde{t}_2}}^2}\right]\right)^2, \tag{5}$$

$$\begin{aligned}
\lambda_{ht_1t_1} &= M_z^2 \cos 2\beta \left(\frac{1}{2}c_t^2 - \frac{2}{3}\sin^2\theta_W \cos 2\theta_t\right) + m_t^2 - s_t^2 c_t^2 ({m_{\tilde{t}_2}}^2 - {m_{\tilde{t}_1}}^2)\,, \\
\lambda_{ht_2t_2} &= M_z^2 \cos 2\beta \left(\frac{1}{2}s_t^2 + \frac{2}{3}\sin^2\theta_W \cos 2\theta_t\right) + m_t^2 + s_t^2 c_t^2 ({m_{\tilde{t}_2}}^2 - {m_{\tilde{t}_1}}^2)\,, \\
A_0[m] &= -[\tau - f(\tau)]\tau^{-2}, \quad f[\tau] = \arcsin^2\sqrt{\tau}, \quad \tau = \frac{m_h}{4\,m^2}, \quad A_{hgg(SM)} \approx 1.38.
\end{aligned} \tag{6}$$

We include the contributions from both stop mass eigenstates, though the contribution from the lighter eigenstate tends to dominate due to the $1/m^2$ factor. LHC data constrain r_{gg} to within $\sim 25\%$ of the SM value [30]. The LHC is expected to probe this quantity to within $12 - 16\%$ $(6 - 10\%)$ of the SM value with 300 fb^{-1} (3000 fb $^{-1}$) of data, whereas the ILC and TLEP can probe it to percent level precision [31]. Such constraints on r_{gg} can therefore result in strong bounds on the stop mixing angle as a function of the two stop masses.

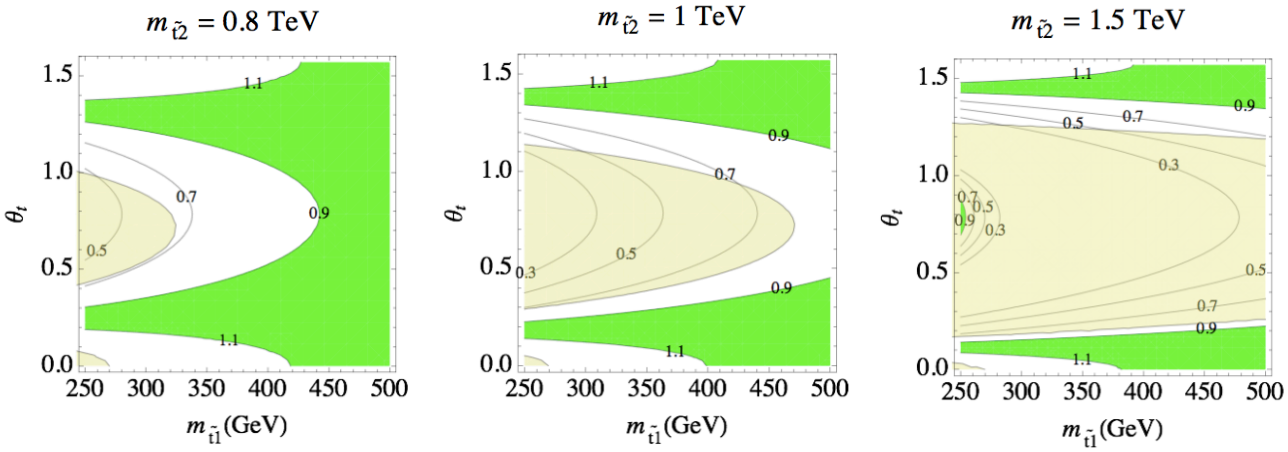

FIG. 3. Contours of r_{gg} as a function of $m_{\tilde{t}_1}$ and the stop mixing angle θ_t, for three choices of $m_{\tilde{t}_2}$: 0.8, 1.0, and 1.5 TeV in the left, center, and right panels. Green regions denote $0.9 \leq r_{gg} \leq 1.1$. Yellow regions denote parameter space incompatible with $\Delta\rho$ constraints.

We illustrate the potential power of such constraints in Fig. 3; future measurements constraining r_{gg} to fall within 10% of its SM value, $0.9 \leq r_{gg} \leq 1.1$, would be compatible with the region shaded in green. The corresponding constraint on the mixing angle becomes stronger as $\tilde{t}_1$ becomes lighter or $\tilde{t}_2$ becomes heavier. Notably, for $m_{\tilde{t}_1} \lesssim 420$ GeV or $\tilde{t}_2 \gtrsim 900$ GeV, the allowed regions of parameter space cleanly separate into two distinct bands corresponding to small and large mixing angles, *i.e.* a mostly left-handed or right-handed $\tilde{t}_1$. We also show regions incompatible with $\Delta\rho$ constraints in yellow, which become stronger as the mass splitting between the stop mass eigenstates increases, as seen earlier in Fig. 2.

In this paper, we work with the most minimal possible spectrum, decoupling all particles other than $\tilde{t}_1, \tilde{t}_2, \tilde{b}_1$, and a bino-like neutralino χ_0, which we take to be the lightest supersymmetric particle (LSP). [2] In all cases, we demand compatibility with both $\Delta\,\rho$ and r_{gg}.

In the next three sections, we demonstrate how the above ideas can be implemented in three distinct scenarios that could be realized at the LHC, corresponding to qualitatively very different signals from $\tilde{t}_1, \tilde{b}_1$, and $\tilde{t}_2$.

[2] Higgsinos are motivated to be light from naturalness considerations. The presence of both light charginos and neutralinos would lead to additional collider signatures. In this paper, for simplicity, we decouple the Higgsinos and keep only a light bino to demonstrate that progress is possible even with this minimal scenario.

III. IMPLICATIONS OF A LIGHT STOP SIGNAL

The latest LHC results impose increasingly stringent constraints on light stops: limits exist for $m_{\tilde{t}_1} \sim m_t + m_\chi$ [6], 3-body decay into $bW\chi_0$ [7], 4-body decay into $bff'\chi_0$ [8], as well as flavor violating decays into $c\chi_0$ [9]. Together, these bounds rule out stop masses below $m_{\tilde{t}_1} \lesssim 250$ GeV (except for small regions). In this section, we therefore focus on the mass window $250 \leq m_{\tilde{t}_1} \leq 500$ GeV, where a light stop is potentially compatible with existing constraints, and discuss the implications of a light stop discovery at the LHC. As laid out in the previous section, the existence of a light stop yields non-trivial constraints from r_{gg}. For this section, we assume the optimistic reach with 300 fb^{-1} of data at the LHC as reported in Ref. [31], which will constrain $0.88 \leq r_{gg} \leq 1.12$.

The constraint on r_{gg} can be mapped onto the physical parameters $m_{\tilde{b}_1}$ and $m_{\tilde{t}_2}$. This is plotted in the top row of Fig. 4, obtained by performing a scan over parameter space, demanding consistency with both $0.88 \leq r_{gg} \leq 1.12$ and $\Delta\rho < 9.6 \times 10^{-4}$. We also find it instructive to look at the mass splittings $\Delta m_{\tilde{b}_1\tilde{t}_1} \equiv m_{\tilde{b}_1} - m_{\tilde{t}_1}$ and $\Delta m_{\tilde{t}_2\tilde{b}_1} \equiv m_{\tilde{t}_2} - m_{\tilde{b}_1}$, which are plotted in the bottom row; the horizontal blue line denotes mass splitting equal to m_W. Points that satisfy $120 \leq m_h \leq 130$ GeV in the MSSM are plotted in green (red) for primarily left-handed (right-handed) $\tilde{t}_1$, while points outside this mass window are shown in gray. We see that while arbitrary $m_{\tilde{b}_1}$ and $m_{\tilde{t}_2}$ can be realized for the mixing angles allowed by r_{gg} and $\Delta\rho$, interesting patterns emerge with the additional requirement of reproducing the Higgs mass. As discussed in the previous section, this imposes an upper limit on $m_{\tilde{t}_2}$ and $m_{\tilde{b}_1}$. It is convenient to separate the discussion into cases where the light stop $\tilde{t}_1$ is mostly left-handed ($\theta_t \leq \pi/4$, green points) or mostly right-handed ($\theta_t \geq \pi/4$, red points).

For mostly left-handed[3] $\tilde{t}_1$, this limit is not very meaningful for $m_{\tilde{t}_2}$, which can be at several TeV (the constraints do impose a *lower* bound on $m_{\tilde{t}_2}$). However, it is sharp for $m_{\tilde{b}_1}$, constraining $\Delta m_{\tilde{b}_1\tilde{t}_1} \lesssim 200$ GeV in the $\tilde{t}_1$ mass window of interest, as seen in the left panels of Fig. 4. In addition to revealing the existence of a light sbottom, these correlations also reveal information about its decay channels: below (above) the m_W line, $\tilde{b}_1$ decays primarily to $b\chi_0$

[3] While additional observations are required to determine whether a stop is left- or right-handed, theoretical considerations may prefer one over the other – for instance, in gauge mediation, the lighter stop is generally left-handed [32].

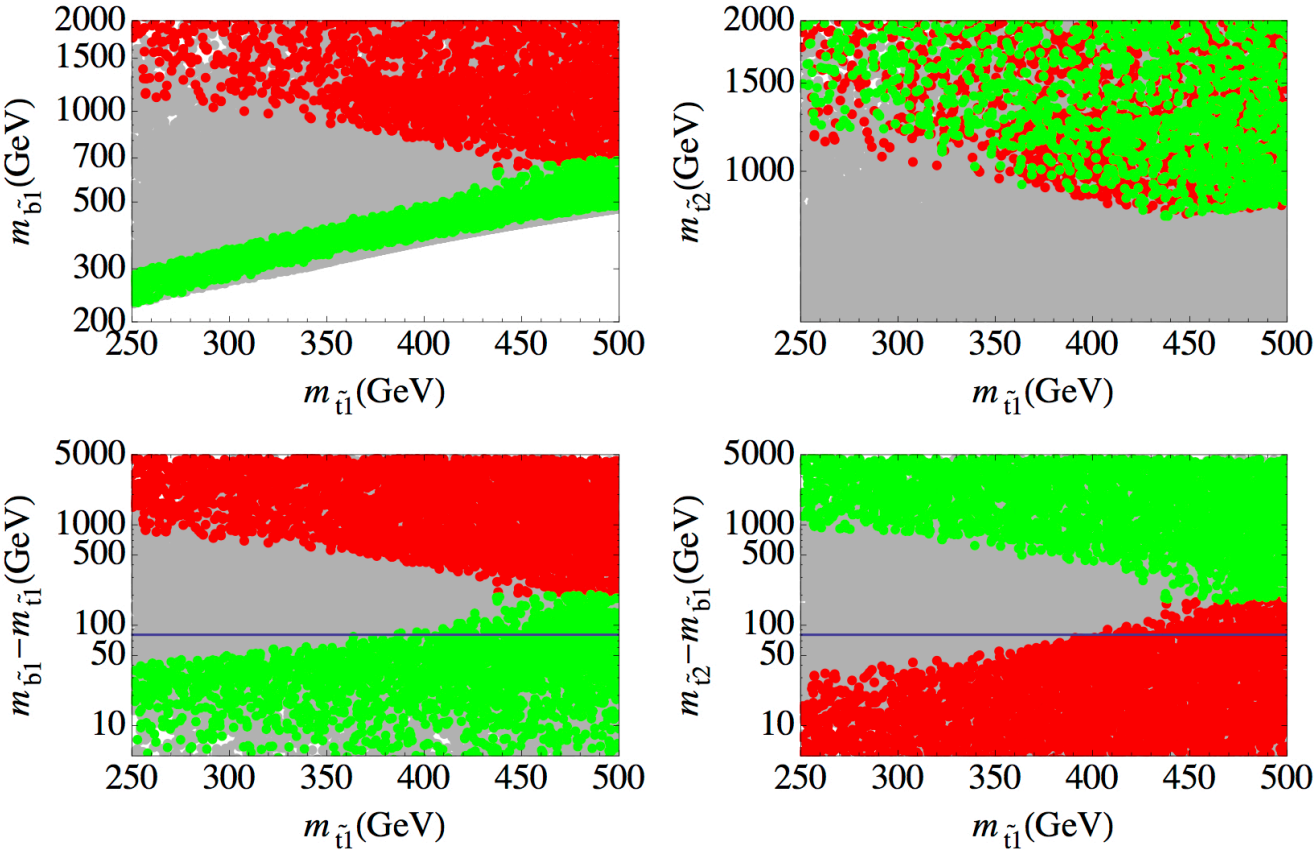

FIG. 4. Masses of sbottom (top left) and heavier stop (top right), and mass splittings between $\tilde{b}_1$ and $\tilde{t}_1$ (bottom left) and between $\tilde{t}_2$ and $\tilde{b}_1$ (bottom right) for light $\tilde{t}_1$ masses. All points are compatible with λ_{hgg} and $\Delta\rho$ constraints. Green (red) points are compatible with $120 \leq m_h \leq 130$ GeV for mostly left-handed (right-handed) $\tilde{t}_1$; grey points have m_h outside this window. The horizontal line in the bottom row corresponds to mass splitting equal to the W boson mass.

$(\tilde{t}_1 W)$.[4] For $m_{\tilde{t}_1} \lesssim 360$ GeV, the relevant splitting is constrained to be smaller than m_W, and the sbottom decays as $\tilde{b}_1 \to b\chi_0$. This decay is strongly constrained by the LHC, with the latest bounds [33–35] ruling out $m_{\tilde{b}_1} \lesssim 900$ GeV for $m_{\chi_0} \lesssim 400$ GeV, effectively eliminating this region ($m_{\tilde{t}_1} \lesssim 360$ GeV) of MSSM parameter space. For $m_{\tilde{t}_1} \gtrsim 360$ GeV, the sbottom can decay primarily as $\tilde{b}_1 \to \tilde{t}_1 W$ if $\Delta m_{\tilde{b}_1\tilde{t}_1} > m_W$, which requires the stops to be split due to large mixing. As argued in the previous section, such large mixings, in turn, enforce strong upper limits on $m_{\tilde{t}_2}$ for compatibility with the MSSM Higgs mass. We find that the $\Delta m_{\tilde{b}_1\tilde{t}_1} > m_W$ region is

[4] We also see points with $m_{\tilde{b}_1} < m_{\tilde{t}_1}$; we do not address them further in this paper.

correlated with $m_{\tilde{t}_2} \lesssim 1.3$ TeV. Such masses are potentially within reach of the 14 TeV LHC, although discovery will be challenging and will require dedicated searches. For a discussion of possible detection strategies in various scenarios, see *e.g.* Ref. [36].

For a mostly right-handed $\tilde{t}_1$, both the $\tilde{b}_1$ and $m_{\tilde{t}_2}$ are heavy ($\gtrsim 700$ GeV; top panels, red points), and searching for their signals is challenging. In this case, the absence of such signals at the LHC does not lead to any meaningful conclusions about the MSSM. In contrast, it is the *lower* bounds on these masses that are relevant. Should a $\tilde{b}_1$ or $\tilde{t}_2$ be discovered with mass lighter than what is shown in the figure, this would be inconsistent with the MSSM, pointing to physics – and contributions to the Higgs mass – beyond the MSSM. [5] For a mostly right-handed $\tilde{t}_1$, the sbottom mass is more closely aligned with the heavier stop mass, and we find $\Delta m_{\tilde{t}_2\tilde{b}_1} \lesssim 200$ GeV (bottom right panel, red points). Moreover, for $m_{\tilde{t}_1} \lesssim 370$ GeV, $\Delta m_{\tilde{t}_2\tilde{b}_1} < m_W$, which implies $\tilde{t}_2 \to \tilde{b}_1 W$ is not allowed in this window, motivating $\tilde{t}_2$ searches in the $\tilde{t}_1 Z$ (and possibly $\tilde{t}_1 h$) channels (we will explore such signals in Sec. V). Likewise, increasing $\Delta m_{\tilde{t}_2\tilde{b}_1} > m_W$, which appears possible for $m_{\tilde{t}_1} \gtrsim 370$ GeV, again requires mixing in the stop sector, resulting in $m_{\tilde{t}_2} \lesssim 1.3$ TeV for compatibility with the Higgs mass in the MSSM, which represents an attractive target for the LHC. In Section IV, we perform a detailed study of a scenario where both $\tilde{b}_1 \to \tilde{t}_1 W$ and $\tilde{t}_2 \to \tilde{b}_1 W$ are open, leading to a multitude of leptonic signals at the LHC.

With the above considerations in mind, we divide our discussion of the interpretations of a $\tilde{t}_1$ signal into three distinct mass windows.

A. $m_{\tilde{t}_1} \sim 300 - 360\ GeV$:

Depending on the LSP mass, a light stop can be discovered at the LHC in this mass window through the 3-body decay $bW\chi_0$, 4-body decay $bff'\chi_0$, or the flavor violating decay $c\chi_0$.

- In the MSSM, if $\tilde{t}_1$ is mostly left-handed, this discovery implies a light sbottom ($m_{\tilde{b}_1} \lesssim 450$ GeV) that decays as $\tilde{b}_1 \to b\chi_0$, which is already ruled out by the latest LHC bounds [33–35]. Discovering such a light stop would therefore imply that either the stop is mostly

[5] A light right-handed sbottom could accidentally exist in the spectrum. Furthermore, we have not considered sizable mixing in the sbottom sector, which could lead to lower sbottom masses than shown in the figure via mixing with the heavier sbottom. There may also be corresponding large contributions to r_{gg} if $\tan\beta$ is large, which must be taken into account.

right-handed (red points) or the underlying theory is not the MSSM (gray points with $\Delta m_{\tilde{b}_1\tilde{t}_1} > m_W$, but with the wrong Higgs boson mass).

- If $\tilde{t}_1$ is mostly right-handed, $\Delta m_{\tilde{t}_2\tilde{b}_1} < m_W$ in the MSSM, and therefore $\tilde{t}_2$ decays primarily to $\tilde{t}_1 Z, \tilde{t}_1 h$. However, both $\tilde{t}_2$ and $\tilde{b}_1$ could be extremely heavy (several TeV) and escape detection.

B. $m_{\tilde{t}_1} \sim 360 - 500\ GeV$:

This heavier stop mass window follows a similar pattern as above, but with the crucial difference that $\tilde{b}_1 \to \tilde{t}_1 W$ (for left-handed $\tilde{t}_1$) and $\tilde{t}_2 \to \tilde{b}_1 W$ (for right-handed $\tilde{t}_1$) can both be kinematically open. These channels can be difficult to probe if the involved mass splittings are not very large. A $\tilde{t}_1$ discovery in this mass window carries the following implications:

- For a mostly left-handed $\tilde{t}_1$, there are two possibilities for the sbottom in the MSSM. If $\tilde{b}_1 \to b\chi_0$, the corresponding $bb + \not{E}_T$ signal, if not observed or ruled out already, should easily be visible at the LHC (see [33–35] for the latest constraints on this channel). If instead $\tilde{b}_1 \to \tilde{t}_1 W$, sbottom discovery may be difficult; however, as discussed earlier, $m_{\tilde{t}_2} \lesssim 1.3$ TeV and might have better detection prospects.

- For a mostly right-handed $\tilde{t}_1$, we can conclude that either $\tilde{t}_2 \to \tilde{b}_1 W$ is not allowed (in this case both $\tilde{t}_2$ and $\tilde{b}_1$ can be very heavy), or $m_{\tilde{t}_2} \lesssim 1.3$ TeV. Note that in this mass window the lower limits on the allowed $\tilde{b}_1$ and $\tilde{t}_2$ masses are also relaxed relative to the lighter stop mass windows (top right panel).

C. $m_{\tilde{t}_1} \lesssim 300\ GeV$:

The latest LHC bounds are extremely stringent in this regime, and require $m_{\tilde{t}_1} \leq m_b + m_W + m_{\chi_0}$. This only allows for the 4-body channel $bff'\chi_0$ or the flavor violating decay into $c\chi_0$, leading to multijet, monojet, or charm-tagged event signals. Compared to the heavier mass windows considered above, a key element of this low mass window is that the bound state of two stops, stoponium [37–44], may also eventually be observed at the LHC. Note that stoponium states are consistent with our choice of a bino LSP, whereas the two-body decay to a chargino and bottom quark prevents the formation of the bound state if the LSP is a wino or higgsino.

A dedicated study in Ref. [45] found that decays of the stopnonium resonance into both $\gamma\gamma$ and γZ channels can be observed at the 14 TeV LHC with 3 ab^{-1} of data for $250 \lesssim m_{\tilde{t}_1} \lesssim 300$ GeV. This enables a very precise measurement of the stop mass, which can then be cross checked with the signal rate in the stop discovery channel. In addition, stoponium signals can crucially also reveal whether the stop is left- or right-handed, since the $\gamma\gamma$ channel can be observed for both left- and right-handed stops, but decays to γZ can only be observed for a mostly left-handed stop [45]. [6] Implications for $\tilde{b}_1$ and $\tilde{t}_2$ masses and decay channels are qualitatively the same as in the $300 - 360$ GeV window discussed above. For a $m_{\tilde{t}_1} \lesssim 300$ GeV stop discovery, the following additional statements can be made:

- A stoponium signal should be observed at the high luminosity LHC with 3/ab of data. The absence of a stoponium signal would point to some physics other than a light $\tilde{t}_1$ as the source of the original (multijet/monojet) signal.

- Observation of stoponium signals in both $\gamma\gamma$ and γZ channels is inconsistent with the MSSM, since the sbottom that accompanies this left-handed stop has already been ruled out by current LHC bounds on $\tilde{b}_1 \to b\chi_0$. Such observations therefore rule out the MSSM as the underlying theory behind these signals.

- Observation of $\gamma\gamma$ only is consistent with a mostly right-handed stop, and implies that the $\tilde{b}_1$ and $\tilde{t}_2$ are above the TeV scale (see top panels in Fig. 4). In this case, observation of a sub-TeV sbottom or second stop would be incompatible with the MSSM.

IV. USING SBOTTOMS TO HELP RECONSTRUCT THE STOP SECTOR

In this section, we discuss how a left-handed sbottom might be observed at the LHC, and how this observation, in conjunction with searches for a heavy stop, might test the MSSM. This strategy can provide successful tests of the MSSM even in the absence of detailed direct information about the lighter stop.

For a predominantly left-handed sbottom, the decay $\tilde{b}_1 \to \tilde{t}_1 W$ dominates if kinematically accessible and $\tilde{t}_1$ has non-negligible left-handed content. For this section, we have in mind a

[6] The stoponium $\gamma\gamma$ channel is observable up to $m_{\tilde{t}_1} \sim 370$ GeV and could therefore be relevant in the heavier mass windows, although this only yields information about the mass and not the handedness.

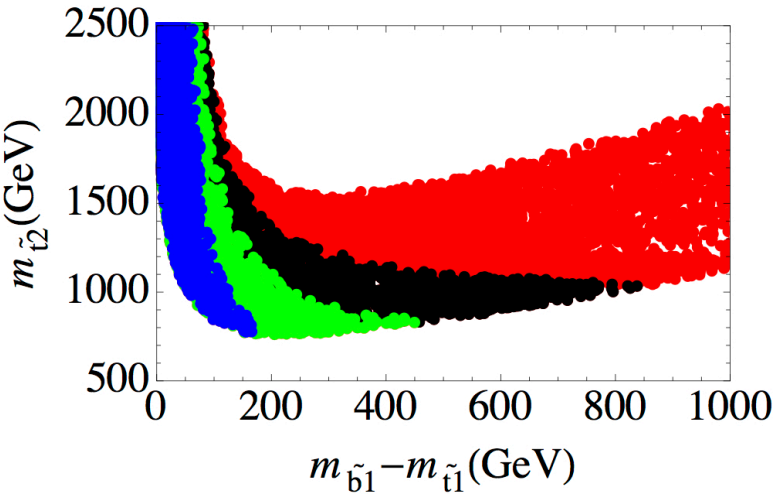

FIG. 5. $m_{\tilde{t}_2}$ as a function of the mass splitting $m_{\tilde{b}_1} - m_{\tilde{t}_1}$ for points with $120 < m_h < 130\,\text{GeV}$ and $m_{\tilde{t}_1} < 1\,\text{TeV}$ in the MSSM. Red, black, green, and blue regions correspond to sbottom masses $m_{\tilde{b}_1} > 1000$, $750 < m_{\tilde{b}_1} < 1000$, $500 < m_{\tilde{b}_1} < 750$, and $m_{\tilde{b}_1} < 500$ GeV respectively.

spectrum where $\tilde{b}_1 \to \tilde{t}_1 W$ and $\tilde{t}_1 \to t\chi_0$, but discovery of direct light stops production is elusive because the spectrum is squeezed. The presence of Ws in the sbottom decay chain suggests that multilepton channels might be a fruitful way to search for such sbottoms. We adopt two search strategies involving leptons as applied at CMS: same-sign dileptons [5] (recently updated in [46]), and a multilepton search strategy [47] (recently updated in [48]), which searches for an excess in $\geq 3\,l$+jets+$\not{E}_T$ at the 13 TeV LHC, and explore whether a sbottom signal can be uncovered with these approaches in the future. [7]

Before exploring the reach of these search strategies, we first discuss the implications of observing such a signal. A multilepton excess interpreted as a $\tilde{b}_1 \to \tilde{t}_1 W$, $\tilde{t}_1 \to t\chi_0$ signal (further corroboration, such as an independent measurements of $\tilde{t}_1$ and the presence of b tags in the excess, will help solidify this interpretation) implies that both $\tilde{t}_1$ and $\tilde{b}_1$ are somewhat left handed (necessary for $\tilde{b}_1 \to \tilde{t}_1 W$ decays), and $\Delta m_{\tilde{b}_1 \tilde{t}_1}$ must be sufficiently large (for the leptons to be hard enough to be observed). Taken together, these imply appreciable mixing in the stop sector, as a purely right-handed $\tilde{t}_1$ precludes this decay channel altogether, while a

[7] CMS analyses do not explicitly interpret their searches using the topology we have in mind ($\tilde{b}_1 \to \tilde{t}_1 W$, $\tilde{t}_1 \to t\chi_0$), but Ref. [47] casts its results in terms of the similar ($\tilde{b} \to t\,\chi^-$, $\chi^- \to W\,\chi_0$), placing the limit $m_{\tilde{b}_1} \lesssim 550$ GeV using 2.3/fb of 13 TeV LHC data. By simulating events for representative benchmark points for the two topologies, we have verified they give similar lepton spectra and $\not{E}_T$ distributions and similar efficiencies (within $\sim 10\%$), for $m_{\tilde{t}_1} \approx m_{\chi^-}$.

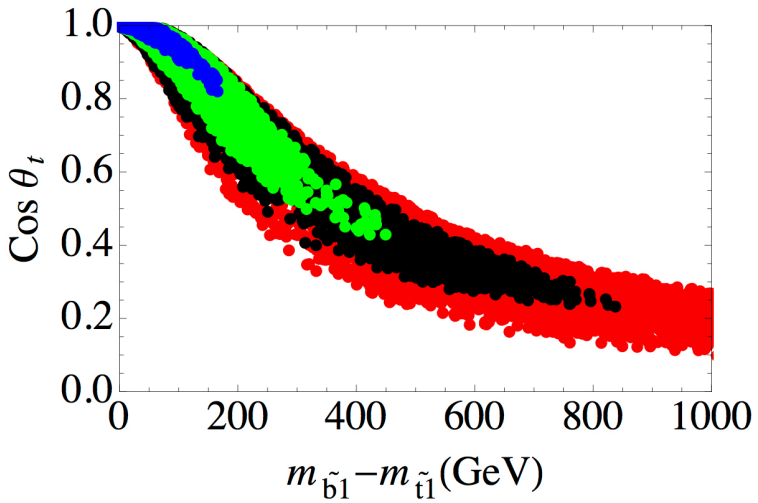

FIG. 6. Cosine of stop mixing angle as a function of the mass splitting $m_{\tilde{b}_1} - m_{\tilde{t}_1}$ for points with $120 < m_h < 130$ GeV and $m_{\tilde{t}_1} < 1$ TeV in the MSSM. Color coding is the same as in Fig. 5.

purely left-handed $\tilde{t}_1$ does not result in a sufficiently large mass splitting with $\tilde{b}_1$.

In the MSSM, these observations have consequences for the second (heavier) stop. We find $m_{\tilde{t}_2}$ is correlated with the $\Delta m_{\tilde{b}_1\tilde{t}_1}$ mass splitting, as shown in Fig. 5 (for $m_{\tilde{t}_1} < 1$ TeV and $120 \leq m_h \leq 130$ GeV in the MSSM as calculated from the 1-loop formula in Eq. (1)). The colored regions (red, black, green, and blue) correspond to different sbottom masses ($m_{\tilde{b}_1} > 1000$, $750 < m_{\tilde{b}_1} < 1000$, $500 < m_{\tilde{b}_1} < 750$, and $m_{\tilde{b}_1} < 500$ GeV respectively). At small $\Delta m_{\tilde{b}_1\tilde{t}_1}$ ($\lesssim 150$ GeV – more difficult to probe via multilepton searches), stop mixing is small, $\tilde{t}_1$ is mostly left-handed, and the desired Higgs mass can be obtained with a heavy (several TeV) $\tilde{t}_2$. The splitting $\Delta m_{\tilde{b}_1\tilde{t}_1}$ can be made larger by increasing the stop mixing angle (this correlation is plotted in Fig. 6); in this case, as discussed in Section II, consistency with the Higgs mass enforces an upper limit on $m_{\tilde{t}_2}$, which is indeed clearly visible in Fig. 5. Alternatively, the splitting can be raised without significant stop mixing by making $\tilde{t}_1$ mostly right-handed; however, in this case, $\tilde{t}_2$ becomes approximately degenerate with $\tilde{b}_1$ and thus again faces an upper mass limit. For large $\Delta m_{\tilde{b}_1\tilde{t}_1}$, there is therefore an upper limit on $m_{\tilde{t}_2}$, which grows stronger for lighter $\tilde{b}_1$, as seen in the various colored bands in Fig. 5. This becomes particularly sharp for a sub-TeV sbottom, which forces $m_{\tilde{t}_2}$ into a narrow wedge-shaped region – for instance, for $m_{\tilde{b}_1} < 750$ GeV and $\Delta m_{\tilde{b}_1\tilde{t}_1} \gtrsim 150\,(200)$ GeV, Fig. 5 tells us that $m_{\tilde{t}_2} \lesssim 1.3\,(1.1)$ TeV.

Thus, the observation of a multilepton+$\not{E}_T$ signal associated with a sub-TeV sbottom and

large $\Delta m_{\tilde{b}_1\tilde{t}_1}$ leads to a robust upper limit on $m_{\tilde{t}_2}$ in the MSSM. These stops may well be within reach of the LHC. Detailed analysis of the multilepton excess can shed further light on the properties of $m_{\tilde{t}_2}$: inferring $\Delta m_{\tilde{b}_1\tilde{t}_1}$ (from, e.g., the lepton p_T distribution) and the sbottom mass (from, e.g., the signal rate) not only narrows the allowed range of $m_{\tilde{t}_2}$ (Fig. 5) but also constrains the stop mixing angle (Fig. 6). It is therefore possible to not only predict a relatively narrow mass window for $\tilde{t}_2$, but also get a profile of its decay channels. Ruling out such a $\tilde{t}_2$ is sufficient to rule out the MSSM.

A TeV scale $\tilde{t}_2$ can be probed in several ways. If it decays primarily via $\tilde{t}_2 \to \tilde{t}_1 Z$, leptonic decays of boosted Z-bosons offer a promising search strategy [49]. For $\tilde{t}_2 \to \tilde{b}_1 W$, the cascade $\tilde{t}_2 \to \tilde{b}_1 W$, $\tilde{b}_1 \to \tilde{t}_1 W$, $\tilde{t}_1 \to t\chi_0$ can produce several high p_T leptons; in this case, there could be excesses in both ≥ 3 and ≥ 4 lepton searches. Likewise, $\tilde{t}_2 \to \tilde{t}_1 h$ can be probed by reconstructing the h with boosted b-jets (see e.g. [50]). Note that even when $\tilde{t}_2 \to \tilde{t}_1 h$ is large, $\tilde{t}_2$ maintains the decay $\tilde{t}_2 \to \tilde{t}_1 Z$, so the search for leptonic Z, boosted hadronic Zs, or a mix of Z and h might be possible.

As an aside, it is important to verify that the original multilepton excess originates primarily from $\tilde{b}_1$ decays rather than from $\tilde{t}_2$ decays. It is possible to be initially fooled: boosted leptons from $\tilde{t}_2$ decays in the blue region of Fig. 5 might mimic a $\tilde{b}_1 \to \tilde{t}_1 W$ signal, leading to the erroneous interpretation that $\Delta m_{\tilde{b}_1\tilde{t}_1}$ is large. However, in such cases, the $\tilde{t}_2$ search strategies discussed in the previous paragraph can reveal the heavier stop, and help clarify the extent to which it might give rise to a multilepton excess.

A. Benchmark Case Study

We choose an MSSM benchmark that produces the correct Higgs boson mass and has third generation squarks below the TeV scale. The masses and branching ratios of the relevant particles, generated with `SUSY-HIT` [18], are listed in Table I. For this spectrum, we simulated 13 TeV LHC collision events with the `Madgraph5_aMC@NLO` package [51], with detector simulation using `Delphes-3.2.0` [52].

Same-sign dileptons search

We first investigate the same-sign dilepton (SSDL) search as discussed in the CMS paper [5]

$\tilde{t}_2:$	$m_{\tilde{t}_2} = 850.9$ GeV,	BR: $\tilde{t}_1 Z$ 77%, $\tilde{b}_1 W$ 18%, $\tilde{t}_1 h$ 3%,	$\sin\theta_t = 0.72$
$\tilde{b}_1:$	$m_{\tilde{b}_1} = 704.6$ GeV,	BR: $\tilde{t}_1 W$ 99.4%	
$\tilde{t}_1:$	$m_{\tilde{t}_1} = 458.6$ GeV,	BR: $t\chi_0$ 100%	
$\chi_0:$	$m_\chi = 239.7$ GeV,	LSP	
$h:$	$m_h = 123.0$ GeV		

TABLE I. Benchmark point: Mass spectrum and branching ratios. For this point, we set $\tan\beta = 15$, $\mu = 800$ GeV, and all other masses (including the gluino mass) to 2 TeV.

(recently updated in [46]), also advocated by a recent study [36] as a promising search strategy for sbottoms. We begin by mirroring the analysis in this CMS paper, imposing the following cuts:

- Require same sign dileptons with $p_T \geq 25$ GeV.
- Impose a Z veto: reject events with opposite sign, same-flavor dilepton pairs with an invariant mass between 76 and 106 GeV.
- Require two or more b-jets, $N_{b-jets} \geq 2$.
- Constrain the missing transverse energy to $200 \leq \not{E}_T \leq 300$ GeV.
- Require $300 \leq H_T \leq 1125$ GeV, where H_T denotes the sum of transverse momenta of all the jets in the event.
- Require 5 or more jets in the event, $N_{jets} \geq 5$.

The resulting number of signal and background events with 300 fb^{-1} of data at the 13 TeV LHC are shown in Table II. The signal primarily results from $\tilde{b}_1$ decays, with $\tilde{t}_2$ decays contributing less than 15% of the signal. The expected background is taken from the CMS analysis [5], scaled up to 300 fb^{-1} of data. We also list the significance of the signal, calculated as $\mathcal{S} \equiv S \,/\, \sqrt{B + \sigma_{bg}^2 B^2}$; the second term in the denominator denotes systematic uncertainties, which are currently around 30% [47], but should improve with future studies and additional data. We calculate the significance for $\sigma_{bg} = 0$, 0.1, and 0.3 to span the range of possibilities.

Search	$\sigma_{\rm prod}$/fb	efficiency(ϵ) ($\times 10^{-4}$)	no. of signal events (S)	background events (B)	$\mathcal{S}$ $\sigma_{bg}=0$	$\mathcal{S}$ $\sigma_{bg}=0.1$	$\mathcal{S}$ $\sigma_{bg}=0.3$
SSDL	-	-	29.4	23.5	6.1	5.4	3.4
$\tilde{b}_1$ contribution	64.2	13	25.0	-	-	-	-
$\tilde{t}_2$ contribution	18.8	8	4.4	-	-	-	-

TABLE II. Same-sign dilepton analysis: Efficiency of cuts, number of events, and significance of signal with 300/fb of data at the 13 TeV LHC. We have defined $\mathcal{S} \equiv S \,/\, \sqrt{B + \sigma_{bg}^2 B^2}$. See text for details.

Our results show that a 3σ signal is possible with the current level of systematic uncertainties with 300 fb^{-1} of data, while an improvement to $\sigma_{bg} = 0.1$ would enable a 5σ discovery.

Multileptons search

Next, we mirror the CMS search for a signal in multileptons (Signal Region (SR) 14, "off-Z" analysis as defined in [47]) by imposing the following set of requirements on the generated event sample (henceforth referred to as "$\geq 3l$offZ"):

- Require three or more electrons or muons with $p_T \geq 20, 15, 10$ GeV.
- Require two or more jets, $N_{jets} \geq 2$.
- Impose a Z veto: reject events with opposite sign, same-flavor dilepton pairs with an invariant mass between 76 and 106 GeV.
- Constrain the missing transverse energy to $50 \leq \not{E}_T \leq 300$ GeV.
- Require $H_T \geq 600$ GeV.

These cuts are not optimized for the signal, but they allow a robust determination of the background as determined by the experiment (which includes a not insignificant contribution from $t\bar{t}$ + fake leptons, which is difficult to estimate via naive simulation). The resulting efficiency of this set of cuts, along with the expected number of signal and background events, and the significance of the signal with 300 fb^{-1} of 13 TeV data is presented in Table III. The expected number of background events is again taken from the CMS analysis [47] and scaled

Search	$\sigma_{\rm prod}$/fb	efficiency(ϵ) ($\times 10^{-4}$)	no. of signal events (S)	background events (B)	$\mathcal{S}$ $\sigma_{bg}=0$	$\mathcal{S}$ $\sigma_{bg}=0.1$	$\mathcal{S}$ $\sigma_{bg}=0.3$
$\geq 3l$offZ	-	-	68.5	240.0	4.4	2.4	0.9
$\tilde{b}_1$ contribution	64.2	31	59.2	-	-	-	-
$\tilde{t}_2$ contribution	18.8	17	9.3	-	-	-	-
$\geq 3l$offZ(II)	-	-	36.8	29.7	6.8	5.9	3.5
$\tilde{b}_1$ contribution	64.2	16	29.9	-	-	-	-
$\tilde{t}_2$ contribution	18.8	12	6.9	-	-	-	-

TABLE III. Multileptons search: Efficiency of cuts, number of events, and significance of signal with 300/fb of data at the 13 TeV LHC. We have defined $\mathcal{S} \equiv S \,/\, \sqrt{B + \sigma_{bg}^2 B^2}$. See text for details.

up to 300 fb^{-1} of data; the paper also lists a detailed breakdown of individual background contributions (see SR14 "off-Z" entries in Table 3 in that paper). We verify `Madgraph5` produces similar results by simulating the ttZ/h background.

Extraction of the signal appears impossible with the current level of systematic uncertainty in background, and challenging even when it is improved to 10%. We can significantly improve the search strategy by modifying the above analysis as follows (denoted as "$\geq 3l$offZ(II)"):

- Reject events with no b-jets. This is particularly effective in suppressing the significant WZ background (see SR14 entry, Table 3 in [47]).
- Require $140 \leq \not{E}_T \leq 300$ GeV instead of $50 \leq \not{E}_T \leq 300$ GeV.

To estimate the background suppression from the b-tag requirement, we look at how individual background contributions drop when this requirement is imposed in the $50 \leq \not{E}_T \leq 300$ GeV, $60 \leq H_T \leq 600$ GeV region – this information is readily available in the CMS analysis [47] (see Table 3, SR 1-12; see Table 1 for their definitions). To estimate the effect of the stronger $\not{E}_T$ cut, we simulate the SM $t\bar{t}Z/h$ background (one of the major backgrounds for this signal), see how it falls for increasing $\not{E}_T$, and make the simplifying assumption that all SM backgrounds scale in the same manner (as noted above, other large backgrounds include $t\bar{t}$ + jets with a fake lepton, which are also expected to fall at large $\not{E}_T$ [47].)

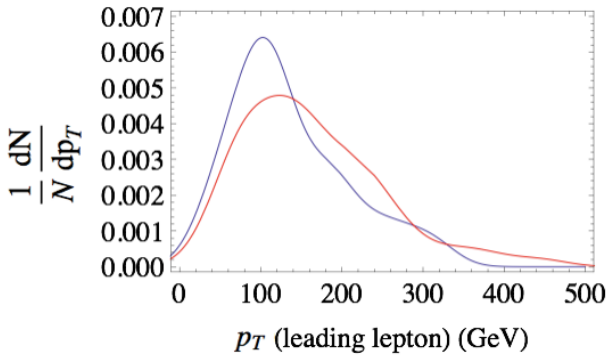

FIG. 7. Comparison of hardest lepton p_T spectra (normalized) for two different mass spectra with mass splittings $m_{\tilde{b}_1} - m_{\tilde{t}_1} = 246$ GeV (red curve) and $m_{\tilde{b}_1} - m_{\tilde{t}_1} = 170$ GeV (blue curve).

The resulting efficiencies, number of events, and signal significance are presented in Table III. These two additional cuts suppress the background by a factor of ~ 10 while rejecting less than half of the signal events. As a result, a 3σ significance is now possible even with the current level of systematic uncertainty in background (30%) with 300 fb^{-1}. Improving it to 10% would enable a 5σ discovery. This search strategy is therefore as efficient as the SSDL analysis in extracting the signal, although a larger fraction of the signal now comes from the heavier stop.

Heavier stop search

As discussed earlier, a light sbottom discovery with a large $\Delta m_{\tilde{b}_1\tilde{t}_1}$ in the MSSM allows us to predict a TeV scale $\tilde{t}_2$. The large mass splitting can be established, for instance, by looking at the p_T spectrum of the hardest lepton. To motivate that it is possible to draw such conclusions, in Fig. 7 we plot, in red, the (normalized) p_T spectrum of the hardest lepton in the signal events in the $\geq 3l$offZ(II) analysis above, which corresponds to $\Delta m_{\tilde{b}_1\tilde{t}_1} = 246$ GeV for our benchmark point. For comparison, we also plot, in blue, the corresponding spectrum for $\Delta m_{\tilde{b}_1\tilde{t}_1} = 170$ GeV. The red spectrum is broader and has a stronger tail (above ~ 330 GeV). By making use of such features, it is plausible that the $\Delta m_{\tilde{b}_1\tilde{t}_1}$ splitting can be determined to within 100 GeV. For our benchmark scenario, this would enable us to predict $m_{\tilde{t}_2} \lesssim 1.2$ TeV. Moreover, this also enables us to deduce that there is significant mixing between the stops (see Fig. 6), and thus Br$(\tilde{t}_2 \to \tilde{t}_1 Z)$ should be significant. The next step, therefore, is to devise a search strategy for such a $\tilde{t}_2$.

Search	$\sigma_{\rm prod}$/fb	efficiency(ϵ) ($\times 10^{-4}$)	no. of signal events (S)	background events (B)	$\mathcal{S}$ $\sigma_{bg}=0$	$\mathcal{S}$ $\sigma_{bg}=0.1$	$\mathcal{S}$ $\sigma_{bg}=0.3$
$>3l$onZ	-	-	48.4	550.4	2.1	0.8	0.3
$\tilde{t}_2$ contribution	18.8	60	34.0	-	-	-	-
$\tilde{b}_1$ contribution	64.2	8	14.4	-	0.6	0.2	0.1
$>3l$onZ(II)	-	-	38.5	43.2	5.9	4.9	2.7
$\tilde{t}_2$ contribution	18.8	47	26.5	-	-	-	-
$\tilde{b}_1$ contribution	64.2	6	12.0	-	1.8	1.5	0.8

TABLE IV. Search 2: Number of events and significance of signal with 300/fb of data at the 13 TeV LHC for the two searches. We have defined $\mathcal{S} \equiv S \,/\, \sqrt{B + \sigma_{bg}^2 B^2}$.

Again, we make use of the CMS analysis as above ($\geq 3l$offZ), except we now require a Z-reconstruction rather than a Z-veto in order to search for Z bosons from $\tilde{t}_2 \to \tilde{t}_1 Z$ decays (this is defined as SR14, "on-Z" analysis in the CMS paper [47]). The background is again taken from the CMS paper [47] (SR14, Table 4) and scaled up to 300 fb^{-1}. We denote this search as "$\geq 3l$onZ", and present the resulting efficiencies, number of events, and signal significance in Table IV. As was the case for the sbottom signal, extraction of the heavier stop signal appears impossible with this unoptimized search. We therefore modify $\geq 3l$onZ as follows (and denote the resulting set of constraints as "$\geq 3l$onZ(II)"):

- Reject events with no b-tagged jets. Again, this is particularly effective in suppressing the dominant WZ background (see SR14 entry, Table 4 in [47]).

- Require $\not{E}_T \geq 200$ GeV instead of $50 \leq \not{E}_T \leq 300$ GeV. Since $\tilde{t}_2$ is significantly heavier than $\tilde{b}_1$, the $\tilde{t}_2$ signal contains a higher $\not{E}_T$ distribution, motivating an even higher $\not{E}_T$ cut than that employed in $\geq 3l$offZ(II).

We estimate the modified background contribution in the same manner as for $\geq 3l$offZ(II). We use information from Table 4, SR 1-12 from [47] to extrapolate the effects of the b-tag requirement on background, and simulate $t\bar{t}Z/h$ to determine the effects of the increased $\not{E}_T$

cut, taking it to be representative of all background. [8] A similar search proposal for $\tilde{t}_2 \to \tilde{t}_1 Z$ in [49] also employed a narrower cut on the Z-boson lepton pair invariant mass as a strategy to suppress background, particularly the combinatoric background from $t\bar{t}$. In the CMS analysis, the $t\bar{t}$ background is claimed to be largely suppressed by the strong $\not{E}_T$ and H_T cuts, hence we do not pursue this strategy in our analysis but note this could provide a further handle.

The results are presented in Table IV. Again, the added cuts prove to be effective in suppressing the background with minimal loss of signal, and we see that a $\sim 3\sigma$ ($\sim 5\sigma$) discovery is possible with existing (improved) systematic uncertainties on the background. For comparison, we also list the signal significance for the sbottom contribution only, which makes it clear that sbottom pollution is minimal.

V. HEAVIER STOP MULTIPLE DECAY CHANNELS IN BOOSTED DIBOSONS

If superpartners are discovered at the LHC, the high luminosity LHC will be able to follow up with measurements in multiple channels with significant statistics. A particularly illustrative example is the decay of the heavier stop $\tilde{t}_2$, which can occur in multiple channels $\tilde{t}_1 Z$, $\tilde{t}_1 h$, $\tilde{b}_1 W$, and $t\chi_0$, with branching ratios determined by the stop masses and mixing angle.

In this section, we focus on the two decays $\tilde{t}_2 \to \tilde{t}_1 Z$ and $\tilde{t}_2 \to \tilde{t}_1 h$, which give rise to boosted dibosons if the mass splitting between the two stop mass eigenstates is large. The tree-level decay widths for these two processes, in the decoupling limit in the Higgs sector are [53]

$$\Gamma(\tilde{t}_2 \to \tilde{t}_1\, Z) = \frac{g^2}{256\pi}\frac{m_{\tilde{t}_2}^3}{m_W^2}\sin^2 2\theta_{\tilde{t}}\,\lambda^{3/2}(1, m_{\tilde{t}_1}^2/m_{\tilde{t}_2}^2, m_Z^2/m_{\tilde{t}_2}^2), \tag{7}$$

$$\Gamma(\tilde{t}_2 \to \tilde{t}_1\, h) = \frac{g^2}{256\pi}\frac{m_{\tilde{t}_2}^3}{M_W^2}|A_h|^2\,\lambda^{3/2}(1, m_{\tilde{t}_1}^2/m_{\tilde{t}_2}^2, m_h^2/m_{\tilde{t}_2}^2),$$

$$A_h = \frac{M_W^2}{m_{\tilde{t}_2}^2}\left(1 - \frac{5}{3}\tan^2\theta_W\right)\sin 2\theta_{\tilde{t}} + \frac{\sin 4\theta_{\tilde{t}}}{2}\left(1 - \frac{m_{\tilde{t}_1}^2}{m_{\tilde{t}_2}^2}\right), \tag{8}$$

where the phase space factor is $\lambda(a,b,c) \equiv a^2 + b^2 + c^2 - 2ab - 2ac - 2bc$. The ratio of the two

[8] Note that $\not{E}_T \geq 300$ GeV is a part of SR15 ($\not{E}_T \geq 300$ GeV, $H_T \geq 600$ GeV) and not SR14 in the CMS analysis [47]. We have appropriately scaled the background in SR15 using results of stronger H_T cuts on our simulated $t\,\bar{t}\,Z/h$ sample to estimate the modified background contribution from this region.

widths is:

$$R_{hZ} \equiv \frac{\Gamma(\tilde{t}_2 \to \tilde{t}_1\, h)}{\Gamma(\tilde{t}_2 \to \tilde{t}_1\, Z)} = \left[\left(1 - \frac{m^2_{\tilde{t}_1}}{m^2_{\tilde{t}_2}}\right)\cos 2\theta_{\tilde{t}} + \frac{m^2_W}{m^2_{\tilde{t}_2}}\left(1 - \frac{5}{3}\tan^2\theta_W\right)\right]^2 \approx \left(1 - \frac{m^2_{\tilde{t}_1}}{m^2_{\tilde{t}_2}}\right)^2 \cos^2 2\theta_{\tilde{t}}. \tag{9}$$

The phase space factors effectively cancel for $m_{\tilde{t}_2} - m_{\tilde{t}_1} \gg m_h, m_Z$. We expect many experimental uncertainties to cancel in this ratio as well. If the two stop masses are known from other measurements, this ratio offers a clean dependence on the stop mixing angle, [9] enabling a check of the MSSM Higgs mass relation. It should be clarified that we are not advocating R_{hZ} as the most precise measurement of the stop mixing angle, but rather as a measurement with a particularly simple dependence on an important parameter in the theory.

An important caveat is that the above expressions only hold at tree level and will be modified by loop corrections to both $\Gamma(\tilde{t}_2 \to \tilde{t}_1\, h)$ and $\Gamma(\tilde{t}_2 \to \tilde{t}_1\, Z)$. The loop corrections are particularly important where the tree level contributions vanish ($\theta \to 0, \pi/2$, for both Eq. (7), (8); Eq. (8) also vanishes for $\theta \to \pi/4$). For parameters that give large $\tilde{t}_2 \to \tilde{t}_1\, h$ and/or $\tilde{t}_2 \to \tilde{t}_1\, Z$ branching ratios (likely necessary for measuring these signals and providing meaningful bounds on the ratio R_{hZ}), loop corrections are generally subdominant. Since loop corrections introduce sensitivity to other supersymmetric parameters (such as the gluino mass), for simplicity, we choose a benchmark where the loop corrections are small and everything can be treated analytically with the relations above. Using the expressions in [54, 55], we estimate that loop contributions can modify R_{hZ} substantially for $\theta_t < 0.1$ and $\theta_t > 1.5$; we therefore exclude these regions in our analysis.[10]

A. Benchmark Case Study

The masses and branching ratios for our chosen benchmark point are listed in Table V; here we computed m_h, $m_{\tilde{b}_1}$, and the $\tilde{t}_2$ branching ratios analytically using formulae listed in the previous sections. We have chosen a point with a large combined branching fraction to Z and h in order to maximize our signal by rendering $\tilde{t}_2 \to \tilde{b}_1 W$ kinematically inaccessible. This

[9] See [16] for similar ideas to extract the stop mixing angle from measurement of ratios of various processes when the Higgsinos are light.

[10] Experimentally, one might be able to confirm that nature is away from these "loop sensitive" windows, either by measurements of r_{gg}, see Fig. 3, or by the absence of $\tilde{t}_2 \to t\chi_0$ decays, which should be present if the branching ratios to $\tilde{t}_1 Z$ and $\tilde{t}_1 h$ are very small.

$\tilde{t}_2:$	$m_{\tilde{t}_2} = 856.9$ GeV,	BR: $\tilde{t}_1 Z$ 53%, $\tilde{t}_1 h$ 30%, $\sin^2\theta_t = 0.987$
$\tilde{b}_1:$	$m_{\tilde{b}_1} = 838.5$ GeV,	decays dominantly to $\tilde{t}_1 W$
$\tilde{t}_1:$	$m_{\tilde{t}_1} = 391.5$ GeV,	decays dominantly to $c\chi_0$
$\chi_0:$	$m_\chi = 371.5$ GeV,	LSP
$h:$	$m_h = 107.0$ GeV	

TABLE V. Mass spectrum and branching ratios for benchmark point.

spectrum results in a too-light Higgs in the MSSM, so a sufficiently precise measurement of such a spectrum would imply additional new physics.

Measuring the ratio R_{hZ} with reasonable precision requires high statistics, motivating searches for the boosted Z and h bosons in their dominant (hadronic) decay channels rather than the cleaner decays into leptons or photons. The prospect of probing such signals by reconstructing the boosted dibosons via fat jets was studied in Ref. [50], which found that a $\sim 4-5\sigma$ discovery of a TeV scale $m_{\tilde{t}_2}$ was possible with 100 fb^{-1} of data at the 14 TeV LHC with a combined diboson signal from $\tilde{t}_2\tilde{t}_2 \to \tilde{t}_1\tilde{t}_1$ + (hZ, ZZ, and hh). For these channels, Ref. [50] estimates a total background cross section (after cuts) of 0.16 fb, dominated by events with two W bosons. With a relatively narrow invariant jet mass window for Higgs boson candidates as in [50], which can further be augmented by jet charge, we estimate that the probability of a "W-jet" faking a "Higgs jet" is very small, likely $< 1\%$ (see Fig. 2(c) in Ref. [56]). Scaling the backgrounds from [50] by this "mistag" probability, we expect the SM backgrounds to be negligible for the hZ and hh channels. Incidentally, we also expect the probability for a Z jet to fake a Higgs jet to be small. R_{hZ} can thus be determined in an essentially background-free environment by considering events with at least one Higgs jet:[11]

$$R_{hZ} \sim \frac{2\, n_{hh}}{n_{Zh}}\,, \tag{10}$$

where n_{ab} denotes the number of signal events where the two boosted dibosons are tagged as a

[11] This strategy also avoids the possibility of contamination from $\tilde{b}_1$ decays with $m_{\tilde{b}_1} \sim m_{\tilde{t}_2}$, where the fat jets from W bosons from $\tilde{b}_1 \to \tilde{t}_1 W$ can be misinterpreted as Z bosons from $\tilde{t}_2 \to \tilde{t}_1 Z$. The $\tilde{b}_1$ contribution was not considered in [50].

	n_{hh}	n_{Zh}	ΔR_{hZ}
300/fb	13	47	0.14
3000/fb	133	469	0.04

TABLE VI. Number of events in each channel and the corresponding uncertainty ΔR_{hZ} for 300 fb^{-1} and 3000 fb^{-1} of data at the 14 TeV LHC. For our benchmark point, $R_{hZ} = 0.57$.

and b. The error in the calculated ratio $R^i_j = n_i/n_j$ is

$$\Delta R^i_j = \sqrt{\left(\frac{\Delta n_i}{n_j}\right)^2 + \left(\frac{n_i \Delta n_j}{n_j^2}\right)^2}. \tag{11}$$

Since the associated backgrounds are negligible, we estimate $\Delta n_i = \sqrt{n_i}$.

Our benchmark point is similar those in Ref. [50] in terms of mass spectra and branching ratios into various decay channels. This allows for a straightforward extrapolation of the results of this study. We extract the signal efficiency from this paper and apply it to our benchmark point, applying a modest correction for the branching ratios. With the simplifying assumption that this analysis is equally efficient in extracting Z and h events (likely approximately true given the nearly identical branching ratios to fully hadronic final states), we estimate an overall (efficiency $\times$ BR) of $\epsilon_{hZ} \approx 6.6 \times 10^{-3}$ and $\epsilon_{hh} \approx 1.8 \times 10^{-3}$. The interested reader is referred to Ref. [50] for details of the analysis.

The resulting number of events and the corresponding uncertainties ΔR_{hZ} are shown in Table VI for 300 fb^{-1} and 3000 fb^{-1} of data at the 14 TeV LHC. For our benchmark point, we find that R_{hZ} can be measured to within $\sim 25\%$ (7%) with 300 (3000) fb^{-1} of data. Whether the fat jet analyses of the type employed here can remain effective in the high luminosity environment is a question for further study.

Next, we discuss how this measurement can shed light on the Higgs boson mass relation and the validity of the MSSM. This requires some knowledge of the two stop masses, hence we assume that $m_{\tilde{t}_1}$ has been measured to lie in the range $350 - 430$ GeV from monojet or charm-tagged events, while $m_{\tilde{t}_2}$ is known to fall in the $800 - 900$ GeV range from various measurements (such as by combining the knowledge of $m_{\tilde{t}_1}$ with information on $p_T(Z)$ in $\tilde{t}_2 \to \tilde{t}_1 Z$ events). The MSSM Higgs mass can then be calculated as a function of θ_t using Eq. (1), which can be

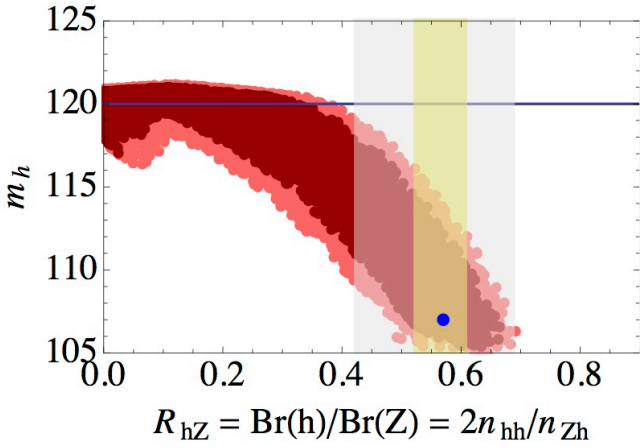

FIG. 8. MSSM Higgs mass as a function of R_{hZ}. The horizontal blue line denotes $m_h = 120$ GeV, the cutoff below which the Higgs mass is taken to be inconsistent with the MSSM. Light (dark) red bands correspond to $350 \leq m_{\tilde{t}_1} \leq 430\,\text{GeV}$ and $800 \leq m_{\tilde{t}_2} \leq 900\,\text{GeV}$ ($360 \leq m_{\tilde{t}_1} \leq 420\,\text{GeV}$ and $815 \leq m_{\tilde{t}_2} \leq 885\,\text{GeV}$). The blue dot denotes the benchmark point in our analysis. Silver and gold bands show uncertainties in the calculated value of R_{hZ} with 300 and 3000 fb^{-1} of data respectively.

converted to a function of the ratio R_{hZ} using Eq. (9). We plot this dependence in Fig. 8 in the broad red band for the above stop mass windows. For comparison, the narrower, darker red band corresponds to $360 \leq m_{\tilde{t}_1} \leq 420$ GeV and $815 \leq m_{\tilde{t}_2} \leq 885$ GeV, and illustrates how the uncertainty in the Higgs mass decreases with better knowledge of the stop masses.

Recall that the Higgs mass is small for vanishing stop mixing $\theta_t \to 0,\ \pi/2$, which corresponds to $R_{hZ} \sim \cos^2 2\theta_t$ approaching 1. On the other hand, achieving the correct Higgs mass with sub-TeV stops requires large stop mixing, which correlates with a smaller value of R_{hZ}. The trend in Fig. 8 is consistent with these observations. Thus, an inferred value of R_{hZ} above some cutoff value R_0 (≈ 0.4 in this case) is incompatible with the MSSM Higgs mass relation. Such an observation would rule out the MSSM, pointing to the need for additional contributions to the Higgs mass.

In the plot, we also show, in the silver (golden) bands, the uncertainties in the calculated value of R_{hZ} for our benchmark point with 300 (3000) fb^{-1} of data. Under our assumptions, exclusion of the MSSM region is borderline with 300 fb^{-1}; however, the MSSM can be clearly excluded with either more data (3000 fb^{-1}, golden band) or better measurements of the stop masses (darker red band). This benchmark study serves as a proof of concept that measure-

ments of the two decay channels $\tilde{t}_2 \to \tilde{t}_1 Z$ and $\tilde{t}_2 \to \tilde{t}_1 h$ can be used as a consistency check of the Higgs mass and possibly rule out the MSSM.

We conclude this section with a few miscellaneous comments. With approximate knowledge of the two stop masses, requiring that r_{gg} remain consistent with observations also constrains the stop mixing angle. For our benchmark point (with the narrower stop mass windows discussed above), we find that r_{gg} measurements at the 300 (3000) fb^{-1} LHC can constrain R_{hZ} to $0.07 < R_{hZ} < 0.67$ $(0.2 < R_{hZ} < 0.6)$, therefore providing complementary handles on the Higgs mass relation. Likewise, if the sbottom has not already been discovered, the above measurements can also be used to predict the mass and decay channels of the sbottom, aiding in its discovery. For our benchmark scenario, the sbottom is degenerate with $\tilde{t}_2$ and decays almost exclusively to $\tilde{b}_1 \to \tilde{t}_1 W$, with $m_{\tilde{t}_1}$ decaying as $\tilde{t}_1 \to c\chi_0$. Dedicated searches optimized towards accepting W jets instead of Z jets might prove fruitful in discovering such a sbottom.

VI. SUMMARY

In this paper, we investigated the implications of a third generation squark signal discovery at the LHC. It is possible to make use of the relation between the stop sector and the Higgs boson mass in the MSSM in a wide variety of scenarios to test the consistency of the MSSM and predict the masses and decay channels of other superpartners, therefore offering clear subsequent targets for the LHC. We elaborated these ideas with studies in three distinct scenarios:

- For a light ($250 \leq m_{\tilde{t}_1} \leq 500$ GeV) stop, constraints on the Higgs-gluon-gluon coupling strongly limit the stop sector parameters, which can be translated into bounds on the $\tilde{b}_1$ and $\tilde{t}_2$ masses, leading to interesting patterns in the MSSM. For instance, the MSSM Higgs mass relation forces $\Delta m_{\tilde{b}_1 \tilde{t}_1} < m_W$ for $m_{\tilde{t}_1} \lesssim 360\,\text{GeV}$ if $\tilde{t}_1$ is left-handed, which is incompatible with current LHC constraints. Likewise, scenarios involving $\tilde{b}_1 \to \tilde{t}_1 W$ or $\tilde{t}_2 \to \tilde{b}_1 W$ require significant stop mixing, and consistency with the Higgs mass in the MSSM leads to the prediction $m_{\tilde{t}_2} \lesssim 1.3$ TeV.

- In the event of a sbottom signal in same-sign dileptons or multileptons+jets+$\not{E}_T$ from $\tilde{b}_1 \to \tilde{t}_1 W$, the correlation between $\Delta m_{\tilde{b}_1 \tilde{t}_1}$ and $m_{\tilde{t}_2}$ in the MSSM can be used to predict the $\tilde{t}_2$ mass and decay channels, thereby aiding $\tilde{t}_2$ searches at the LHC.

- For fixed stop masses, the ratio of $\tilde{t}_2 \to \tilde{t}_1 Z$ and $\tilde{t}_2 \to \tilde{t}_1 h$ decay widths is determined by the stop mixing angle, and measuring this ratio with sufficient precision can test the MSSM Higgs mass relation and therefore check the validity of the MSSM. We illustrated the plausibility of this scenario with a case study of the reconstruction of the boosted dibosons from fat jets at the high luminosity LHC with 3/ab of data.

These examples do not cover the full range of signals or spectra that are possible in the MSSM, and it might also be interesting to perform similar studies focusing on signals involving, *e.g.*, light Higgsinos or the gluino. Likewise, we employed several approximations in our studies. Higher precision calculations and more careful simulations would be warranted should a relevant signal actually be discovered at the LHC. Nevertheless, the scenarios we studied here illustrate the power and applicability of the Higgs mass relation in unravelling the supersymmetric sector.

ACKNOWLEDGMENTS

We thank Bob Zheng for valuable discussions and collaboration in the early stages of this project. We also acknowledge helpful discussions with Haipeng An, Diptimoy Ghosh, Nausheen Shah, and Carlos Wagner. This work is supported by the U.S. Department of Energy, Office of Science, under grant DE-SC0007859. BS also acknowledges support from the University of Cincinnati. This work was performed in part at the Aspen Center for Physics, which is supported by National Science Foundation grant PHY-1066293.

---

[1] M. Aaboud *et al.* (ATLAS), (2016), arXiv:1606.03903 [hep-ex].

[2] G. Aad *et al.* (ATLAS), Eur. Phys. J. **C75**, 510 (2015), [Erratum: Eur. Phys. J.C76,no.3,153(2016)], arXiv:1506.08616 [hep-ex].

[3] V. Khachatryan *et al.* (CMS), (2016), arXiv:1605.08993 [hep-ex].

[4] *Search for direct production of top squark pairs decaying to all-hadronic final states in pp collisions at sqrt(s) = 13 TeV*, Tech. Rep. CMS-PAS-SUS-16-007 (CERN, Geneva, 2016).

[5] V. Khachatryan *et al.* (CMS), (2016), arXiv:1605.03171 [hep-ex].

[6] *Search for the Supersymmetric Partner of the Top Quark in the Jets+Emiss Final State at sqrt(s) = 13 TeV*, Tech. Rep. ATLAS-CONF-2016-077 (CERN, Geneva, 2016).

[7] *Search for direct top squark pair production and dark matter production in final states with two leptons in $\sqrt{s} = 13$ TeV pp collisions using 13.3 fb^{-1} of ATLAS data*, Tech. Rep. ATLAS-CONF-2016-076 (CERN, Geneva, 2016).

[8] *Search for direct top squark pair production in the fully hadronic final state in proton-proton collisions at sqrt(s) = 13 TeV corresponding to an integrated luminosity of 12.9/fb*, Tech. Rep. CMS-PAS-SUS-16-029 (CERN, Geneva, 2016).

[9] M. Aaboud *et al.* (ATLAS), (2016), arXiv:1604.07773 [hep-ex].

[10] J. H. Collins, J. A. Dror, and M. Farina, Phys. Rev. **D92**, 095022 (2015), arXiv:1508.02419 [hep-ph].

[11] P. Huang, A. Ismail, I. Low, and C. E. M. Wagner, Phys. Rev. **D92**, 075035 (2015), arXiv:1507.01601 [hep-ph].

[12] J. R. Ellis, G. Ridolfi, and F. Zwirner, Phys. Lett. **B257**, 83 (1991).

[13] H. E. Haber and R. Hempfling, Phys. Rev. Lett. **66**, 1815 (1991).

[14] Y. Okada, M. Yamaguchi, and T. Yanagida, Prog. Theor. Phys. **85**, 1 (1991).

[15] M. Carena, P. H. Chankowski, S. Pokorski, and C. E. M. Wagner, Phys. Lett. **B441**, 205 (1998), arXiv:hep-ph/9805349 [hep-ph].

[16] K. Rolbiecki, J. Tattersall, and G. Moortgat-Pick, Eur. Phys. J. **C71**, 1517 (2011), arXiv:0909.3196 [hep-ph].

[17] S. P. Martin, (1997), [Adv. Ser. Direct. High Energy Phys.18,1(1998)], arXiv:hep-ph/9709356 [hep-ph].

[18] A. Djouadi, M. M. Muhlleitner, and M. Spira, *Physics at LHC. Proceedings, 3rd Conference, Cracow, Poland, July 3-8, 2006*, Acta Phys. Polon. **B38**, 635 (2007), arXiv:hep-ph/0609292 [hep-ph].

[19] J. Pardo Vega and G. Villadoro, JHEP **07**, 159 (2015), arXiv:1504.05200 [hep-ph].

[20] P. Draper, G. Lee, and C. E. M. Wagner, Phys. Rev. **D89**, 055023 (2014), arXiv:1312.5743 [hep-ph].

[21] G. Lee and C. E. M. Wagner, Phys. Rev. **D92**, 075032 (2015), arXiv:1508.00576 [hep-ph].

[22] G. Degrassi, P. Slavich, and F. Zwirner, Nucl. Phys. **B611**, 403 (2001), arXiv:hep-ph/0105096 [hep-ph].

[23] R. Barbieri and L. Maiani, Nucl. Phys. **B224**, 32 (1983).

[24] C. S. Lim, T. Inami, and N. Sakai, Phys. Rev. **D29**, 1488 (1984).

[25] M. Drees and K. Hagiwara, Phys. Rev. **D42**, 1709 (1990).

[26] S. Heinemeyer, W. Hollik, and G. Weiglein, Phys. Rept. **425**, 265 (2006), arXiv:hep-ph/0412214 [hep-ph].

[27] V. Barger, P. Huang, M. Ishida, and W.-Y. Keung, Phys. Lett. **B718**, 1024 (2013), arXiv:1206.1777 [hep-ph].

[28] A. Djouadi, Phys. Rept. **457**, 1 (2008), arXiv:hep-ph/0503172 [hep-ph].

[29] A. Djouadi, Phys. Rept. **459**, 1 (2008), arXiv:hep-ph/0503173 [hep-ph].

[30] G. Aad *et al.* (ATLAS, CMS), (2016), arXiv:1606.02266 [hep-ex].

[31] S. Dawson *et al.*, in *Proceedings, Community Summer Study 2013: Snowmass on the Mississippi (CSS2013): Minneapolis, MN, USA, July 29-August 6, 2013* (2013) arXiv:1310.8361 [hep-ex].

[32] S. Knapen and D. Redigolo, (2016), arXiv:1606.07501 [hep-ph].

[33] *An inclusive search for new phenomena in final states with one or more jets and missing transverse momentum at 13 TeV with the AlphaT variable*, Tech. Rep. CMS-PAS-SUS-16-016 (CERN, Geneva, 2016).

[34] *Search for new physics in the all-hadronic final state with the MT2 variable*, Tech. Rep. CMS-PAS-SUS-16-015 (CERN, Geneva, 2016).

[35] *Search for supersymmetry in events with jets and missing transverse momentum in proton-proton collisions at 13 TeV*, Tech. Rep. CMS-PAS-SUS-16-014 (CERN, Geneva, 2016).

[36] H.-C. Cheng, L. Li, and Q. Qin, (2016), arXiv:1607.06547 [hep-ph].

[37] P. Moxhay and R. W. Robinett, Phys. Rev. **D32**, 300 (1985).

[38] M. J. Herrero, A. Mendez, and T. G. Rizzo, Phys. Lett. **B200**, 205 (1988).

[39] V. D. Barger and W.-Y. Keung, Phys. Lett. **B211**, 355 (1988).

[40] K. Hagiwara, K. Kato, A. D. Martin, and C. K. Ng, Nucl. Phys. **B344**, 1 (1990).

[41] M. Drees and M. M. Nojiri, Phys. Rev. **D49**, 4595 (1994), arXiv:hep-ph/9312213 [hep-ph].

[42] S. P. Martin, Phys. Rev. **D77**, 075002 (2008), arXiv:0801.0237 [hep-ph].

[43] S. P. Martin and J. E. Younkin, Phys. Rev. **D80**, 035026 (2009), arXiv:0901.4318 [hep-ph].

[44] J. E. Younkin and S. P. Martin, Phys. Rev. **D81**, 055006 (2010), arXiv:0912.4813 [hep-ph].

[45] B. Batell and S. Jung, JHEP **07**, 061 (2015), arXiv:1504.01740 [hep-ph].

[46] *Search for SUSY in same-sign dilepton events at 13 TeV*, Tech. Rep. CMS-PAS-SUS-16-020 (CERN, Geneva, 2016).

[47] *Search for SUSY with multileptons in 13 TeV data*, Tech. Rep. CMS-PAS-SUS-16-003 (CERN, Geneva, 2016).

[48] *Search for SUSY with multileptons in 13 TeV data*, Tech. Rep. CMS-PAS-SUS-16-022 (CERN, Geneva, 2016).

[49] M. Perelstein and C. Spethmann, JHEP **04**, 070 (2007), arXiv:hep-ph/0702038 [hep-ph].

[50] D. Ghosh, Phys. Rev. **D88**, 115013 (2013), arXiv:1308.0320 [hep-ph].

[51] J. Alwall, R. Frederix, S. Frixione, V. Hirschi, F. Maltoni, O. Mattelaer, H. S. Shao, T. Stelzer, P. Torrielli, and M. Zaro, JHEP **07**, 079 (2014), arXiv:1405.0301 [hep-ph].

[52] J. de Favereau, C. Delaere, P. Demin, A. Giammanco, V. Lematre, A. Mertens, and M. Selvaggi (DELPHES 3), JHEP **02**, 057 (2014), arXiv:1307.6346 [hep-ex].

[53] H. Baer and X. Tata, *Weak scale supersymmetry: From superfields to scattering events* (Cambridge University Press, 2006).

[54] A. Bartl, H. Eberl, K. Hidaka, S. Kraml, W. Majerotto, W. Porod, and Y. Yamada, Phys. Rev. **D59**, 115007 (1999), arXiv:hep-ph/9806299 [hep-ph].

[55] A. Bartl, H. Eberl, K. Hidaka, S. Kraml, W. Majerotto, W. Porod, and Y. Yamada, Phys. Lett. **B419**, 243 (1998), arXiv:hep-ph/9710286 [hep-ph].

[56] G. Aad *et al.* (ATLAS), Eur. Phys. J. **C76**, 238 (2016), arXiv:1509.04939 [hep-ex].